

---

# NEURAL NETWORKS WITH ORTHOGONAL JACOBIAN

---

**Alex Massucco**

Department of Applied Mathematics  
and Theoretical Physics,  
University of Cambridge, Cambridge, UK  
`am3270@cam.ac.uk`

**Davide Murari**

Department of Applied Mathematics  
and Theoretical Physics,  
University of Cambridge, Cambridge, UK  
`dm2011@cam.ac.uk`

**Carola-Bibiane Schönlieb**

Department of Applied Mathematics  
and Theoretical Physics,  
University of Cambridge, Cambridge, UK  
`cbs31@cam.ac.uk`

## Abstract

Very deep neural networks achieve state-of-the-art performance by extracting rich, hierarchical features. Yet, training them via backpropagation is often hindered by vanishing or exploding gradients. Existing remedies—such as orthogonal or variance-preserving initialisation and residual architectures—allow for a more stable gradient propagation and the training of deeper models. In this work, we introduce a unified mathematical framework that describes a broad class of nonlinear feedforward and residual networks, whose input-to-output Jacobian matrices are exactly orthogonal almost everywhere. Such a constraint forces the resulting networks to achieve perfect dynamical isometry and train efficiently despite being very deep. Our formulation not only recovers standard architectures as particular cases but also yields new designs that match the trainability of residual networks without relying on conventional skip connections. We provide experimental evidence that perfect Jacobian orthogonality at initialisation is sufficient to stabilise training and achieve competitive performance. We compare this strategy to networks regularised to maintain the Jacobian orthogonality and obtain comparable results. We further extend our analysis to a class of networks well-approximated by those with orthogonal Jacobians and introduce networks with Jacobians representing partial isometries. These generalized models are then showed to maintain the favourable trainability properties.

## 1 Introduction

Neural networks can provide very accurate approximations of unknown functions, and their theoretical expressive power tends to grow as they get deeper [37, 51]. Deep neural networks can extract hierarchical features from the input data, allowing for more efficient solutions to challenging approximation problems, such as image classification. On the other hand, deeper networks are more difficult to train using the backpropagation algorithm due to instability issues in gradient propagation [20]. To address this problem, several solutions have been proposed. Residual neural networks (ResNets) were introduced in [18] as a strategy to improve the trainability of deeper models. Thanks to their skip connections, they display reduced vanishing and exploding gradient issues [3, 13]. The key variation proposed in [18] is to modify the layers of a feedforward network (FF) from having form  $x \mapsto F_{\theta_i}(x)$  to  $x \mapsto x + F_{\theta_i}(x)$ .

The idea that skip-connections are the only way to make deeper networks trainable, whereas very deep feedforward networks cannot be trained, was challenged by several researchers. In [40], the authors study the learning dynamics of deep linear networks. They demonstrate that initialising the network weights as

orthogonal matrices allows for depth-independent learning times and to train models that would not be trainable with Gaussian initialisations. In [40], the notion of *dynamical isometry* is introduced, referring to a situation where the singular values of the network Jacobian are all clustered around one. The notion of dynamical isometry has attracted considerable attention, allowing for the training of extremely deep convolutional neural networks without residual connections [49]. Linear neural networks achieve perfect Jacobian orthogonality when they have orthogonal weights. In contrast, for non-linear networks, one generally looks for approximate dynamical isometry, meaning that the singular values are all close to one. In [36], the authors study how the distribution of singular values changes with different choices of activation functions, arguing that feedforward networks based on the ReLU activation function cannot achieve the dynamical isometry.

## Main contributions

This paper presents a unifying framework to describe a broad class of non-linear neural networks that can achieve perfect orthogonality in their Jacobian matrices. Our mathematical description allows us to recover feedforward and residual networks, and derive new neural architectures that are as simple to train as conventional ResNets. Our mathematical derivations clarify that to achieve perfect Jacobian orthogonality, a precise connection between the activation function and the form of the skip connection must exist. We also characterise the links between Jacobian orthogonality and networks with unit Lipschitz constants, as all the networks we construct satisfy this condition and could hence be used to get improved adversarial robustness or in several other contexts. Furthermore, we propose a weakened notion of orthogonality and numerically demonstrate the trainability of such models. We then identify a set of limiting functions, not necessarily with orthogonal Jacobians, that can be approximated to arbitrary accuracy with our network layers with orthogonal Jacobian. We furthermore bring numerical evidence that these limit architectures inherit the good trainability properties.

While perfect Jacobian orthogonality can sometimes be desirable, achieving it only at initialisation is often sufficient to improve network trainability. We support these claims with illustrative numerical experiments aiming at classifying the images of the Fashion MNIST dataset.

## Related works

**Vanishing and exploding gradients.** Skip-connections and the dynamical isometry property are not the only approaches to handle vanishing and exploding gradients. Another approach is to modify the architecture to have a Jacobian matrix with a lower-bounded norm. Two examples are Hamiltonian Neural Networks [30, 12, 15] and reversible neural networks [46]. Architectural changes are not limited to those mentioned above, and one of the most effective insights in improving the ability to train deeper networks has been the introduction of gating mechanisms, for example, in LSTMs [21], or in Highway networks [43]. Another common strategy to improve gradient stability is layer normalisation, which centres and rescales activations at each layer, keeping gradient magnitudes in a healthy range [23, 2, 48]. Activation functions are one of the primary sources of vanishing gradients. Thus, there has been considerable research effort in designing and studying well-behaved activation functions such as SeLU [26], ReLU or LeakyReLU [50, 29]. Similarly, in [1], the authors design the GroupSort activation function that has an orthogonal Jacobian, but which is not applied entrywise. On the other hand, a practical remedy for exploding gradients is gradient clipping [35].

**Jacobian orthogonality and Lipschitz constraints.** Jacobian orthogonality is often a consequence of weight orthogonality. This constraint has attracted considerable interest not only for the network trainability but also for constraining the Lipschitz constant of a network [47, 42, 44]. Networks with limited Lipschitz constant display improved adversarial robustness [45, 41, 44, 38, 31], are fundamental for generative modelling [14, 32, 28], and lead to converging data-driven algorithms in inverse problems [41, 39, 19].

**Functions with orthogonal Jacobian almost everywhere.** Networks with orthogonal Jacobians are not so popular in deep learning. Still, the Jacobian constraint has attracted considerable interest in other areas of mathematics. We mention [8, 6, 9, 5], where the authors study this condition in the context of origami and folding problems through the lens of partial differential inclusions. This analysis has applications in the theory of plates [25, 7]. The theory in the aforementioned works is rather general and relies on minimal assumptions. In contrast, we provide a constructive, self-contained analysis tailored to map resembling conventional neural networks, which admit efficient implementation.

**Piecewise-linear activation functions.** All of our constructions rely on piecewise-linear activation functions, among which we identify specific choices that allow for networks with orthogonal Jacobians. This class of activation functions have the benefit of being easier to analyse mathematically, and we adopt them in connection with isometries. Several variations of the conventional ReLU and LeakyReLU activations have been proposed in the literature. Of interest to our work are learnable activations, such as the Parametric ReLU (PReLU) activation function in [17] where the slope of LeakyReLU is trainable, or activations with several more trainable parameters, such as those proposed in [53, 24, 4].

## Outline of the paper

The paper is organised as follows. Section 2 presents the mathematical framework for a general class of neural networks with orthogonal Jacobian and introduces a weakened notion of orthogonality, which we conjecture to generalise the previous, stronger assumptions. In Section 3, we deduce some examples from the general formulation, proving the ability of our framework to capture original and well-known architectures. Section 4 is then devoted to the analysis of the theoretical approximation properties of our network class. This paper is primarily theoretical. Still, in Section 5, we demonstrate the effectiveness of the proposed architectures for classification tasks. We provide empirical evidence that our networks train efficiently, despite being very deep. We also demonstrate that orthogonality at initialisation is often sufficient for model trainability. The paper concludes with Section 6, where we summarise our findings and discuss their value and future developments.

## Notation

We will denote with  $\mathcal{O}(n)$  the set of  $n \times n$  orthogonal matrices  $\mathcal{O}(n) = \{A \in \mathbb{R}^{n \times n} \mid A^\top A = A A^\top = I_n\}$ , where  $I_n \in \mathbb{R}^{n \times n}$  denotes the identity matrix, and write  $1_n \in \mathbb{R}^n$  to indicate a vector of ones. For a vector field  $F : \mathbb{R}^n \rightarrow \mathbb{R}^n$  which is almost everywhere differentiable, we denote with  $F'(x) \in \mathbb{R}^{n \times n}$  its Jacobian at  $x$ , which is well defined for almost every  $x \in \mathbb{R}^{n \times n}$ . Moreover, we denote with  $\sigma(\cdot; \alpha, \beta) : \mathbb{R} \rightarrow \mathbb{R}$  a Lipschitz continuous function with derivative in the set  $\{\alpha, \beta\}$ ,  $\alpha, \beta \in \mathbb{R}$ , almost everywhere (a.e.). Finally, for a given a subset  $\Omega_i \subset \mathbb{R}^n$ ,  $1_{\Omega_i} : \mathbb{R}^n \rightarrow \mathbb{R}$  denotes its indicator function, i.e.,  $1_{\Omega_i}(x) = 1$  if  $x \in \Omega_i$  and vanishes otherwise.  $\bar{\Omega}_i$  stands for the closure of  $\Omega_i$ .

## 2 Theoretical characterisation

We now provide a characterisation of a broad class of vector fields with an orthogonal Jacobian matrix for almost every input  $x \in \mathbb{R}^n$ . The vector fields we consider are defined based on partitioning the input space  $\mathbb{R}^n$  into open and connected sets. Lemma 2.4 shows that, when the vector field is sufficiently regular, it has an orthogonal Jacobian matrix almost everywhere if and only if it is piecewise affine. We then focus on a family of parametric vector fields resembling commonly implemented neural networks. In Theorem 2.6, we show how to constrain those neural networks to have an orthogonal Jacobian matrix for almost every input.

The vector fields considered in this section may exhibit jump discontinuities. Then, given the growing interest in networks with discontinuous dynamics (e.g., [27, 10, 52]), we emphasize that our results can also be applied and be practically relevant to this broader class of systems.

**DEFINITION 2.1.** Let  $\Omega \subseteq \mathbb{R}^n$  be a closed connected set and  $N \in \mathbb{N}$ . We say that  $\{\Omega_i\}_{i \in [1, N]}$  belongs to  $\mathcal{P}(\Omega)$  if:

- i.  $\Omega_1, \dots, \Omega_N \subset \Omega$  are disjoint open and connected sets,
- ii.  $\Omega = \bigcup_{i=1}^N \bar{\Omega}_i$ ,
- iii.  $\partial \bar{\Omega}_1, \dots, \partial \bar{\Omega}_N$  are Lipschitz boundaries with zero  $n$ -dimensional Lebesgue measure.

We now report a fundamental definition, which can be found in [8, Definition 2.2].

**DEFINITION 2.2** (Piecewise  $C^1$  map). Let  $F : \Omega \subseteq \mathbb{R}^n \rightarrow \mathbb{R}^n$  be Lipschitz continuous. Let  $\Sigma \subset \Omega$  be the set of points where  $F$  is not differentiable.  $F$  is piecewise  $C^1$  if (i)  $\Sigma$  is closed in  $\Omega$ , (ii)  $F$  is continuously differentiable on the connected components of  $\Omega \setminus \Sigma$ , and (iii) for any compact set  $K \subset \Omega$ , the number of connected components of  $\Omega \setminus \Sigma$  intersecting  $K$  is finite.

**DEFINITION 2.3** (Piecewise affine). Let  $F : \Omega \subseteq \mathbb{R}^n \rightarrow \mathbb{R}^n$  be Lipschitz continuous and piecewise  $C^1$ . We say that  $F$  is piecewise affine, and we write  $F \in \mathcal{A}$ , if it is affine on every connected component of  $\Omega \setminus \Sigma$ , where  $\Sigma$  is the non-differentiability set of  $F$ .

**LEMMA 2.4.** Let  $\{\Omega_i \subseteq \mathbb{R}^n \mid i = 1, \dots, N\}$  be a collection of sets in  $\mathcal{P}(\Omega)$ , with  $\Omega \subseteq \mathbb{R}^n$  connected. Consider a vector field  $F : \mathbb{R}^n \rightarrow \mathbb{R}^n$  whose restriction to  $\Omega_i$ , which we call  $F_i : \Omega_i \rightarrow \mathbb{R}^n$ , is piecewise  $C^1$  for every  $i = 1, \dots, N$ . Then,  $F'(x) \in \mathcal{O}(n)$  for almost every  $x \in \Omega$  if and only if  $F_1, \dots, F_N$  are piecewise affine.

We omit the proof of this lemma, since it can be found in [8, Lemma 4.1].

Let us now focus on maps resembling commonly implemented neural network layers. We consider a particular class of functions  $F : \Omega \subseteq \mathbb{R}^n \rightarrow \mathbb{R}^n$  of the form

$$F(x) = \sum_{i=1}^N 1_{\Omega_i}(x) (g_i(x) + d_i A^\top \sigma_i(Bx + b)) \quad (2.1)$$

where  $\{\Omega_1, \dots, \Omega_N\}$  is in  $\mathcal{P}(\Omega)$ ,  $A, B \in \mathbb{R}^{n \times n}$ ,  $b \in \mathbb{R}^n$ , and  $d_i \in \mathbb{R} \setminus \{0\}$ . We assume that, for every  $i = 1, \dots, N$ ,  $g_i(x) = \ell_i x + c_i$  with  $\ell_i, c_i \in \mathbb{R}$ , and  $\sigma_i : \mathbb{R} \rightarrow \mathbb{R}$  is a piecewise  $C^1$  Lipschitz continuous scalar function applied entrywise. We now characterise how  $A$ ,  $B$ , and the activation functions  $\sigma_1, \dots, \sigma_N : \mathbb{R} \rightarrow \mathbb{R}$  need to be chosen for  $F$  to have an orthogonal Jacobian almost everywhere, whatever the partition  $\{\Omega_1, \dots, \Omega_N\}$  under consideration.

We remark that if, for example,  $N = 1$ ,  $\Omega = \mathbb{R}^n$ ,  $g_1(x) = x$ , and  $\sigma_1(x) = \text{ReLU}(x)$ , we recover a rather standard ResNet layer  $F(x) = x + A^\top \text{ReLU}(Bx + b)$ , whereas if  $N = 1$ ,  $\Omega = \mathbb{R}^n$ ,  $g_1(x) = 0$ , and  $\sigma_1(x) = \text{ReLU}(x)$  we recover the feedforward network layer  $F(x) = A^\top \text{ReLU}(Bx + b)$ . We will return to these examples in Section 3.

We now define a set of functions fundamental to our derivation, and then present the first main result of the paper.

**DEFINITION 2.5.** We denote with  $\mathcal{L}(\alpha, \beta)$  the set of scalar piecewise affine and continuous functions with slopes  $\alpha, \beta \in \mathbb{R}$ :

$$\mathcal{L}(\alpha, \beta) = \{\sigma : \mathbb{R} \rightarrow \mathbb{R} : \sigma'(x) \in \{\alpha, \beta\} \text{ a.e.}\} \cap \mathcal{A} \cap C,$$

where  $C$  is the space of continuous functions.

**THEOREM 2.6.** Let  $N \in \mathbb{N}$  and  $\{\Omega_1, \dots, \Omega_N\}$  in  $\mathcal{P}(\mathbb{R}^n)$  be arbitrary. Consider  $F : \mathbb{R}^n \rightarrow \mathbb{R}^n$  defined as in (2.1), with  $\sigma_i : \mathbb{R} \rightarrow \mathbb{R}$  Lipschitz continuous and piecewise  $C^1$ , and  $g_i(x) = \ell_i x + c_i$ ,  $\ell_i, c_i \in \mathbb{R}$ , for every  $i = 1, \dots, N$ . Then,  $F'(x)$  is orthogonal for almost every  $x \in \mathbb{R}^n$  if and only if either

- (i)  $A, B \in \mathcal{O}(n)$ ,  $g_i(x) = c_i \in \mathbb{R}$ , and  $\sigma_i \in \mathcal{L}\left(-\frac{1}{d_i}, \frac{1}{d_i}\right)$ , for any  $i = 1, \dots, N$ , or
- (ii)  $A = B \in \mathcal{O}(n)$ ,  $g_i(x) = \ell_i x + c_i$ , with  $\ell_i, c_i \in \mathbb{R}$ , and  $\sigma_i \in \mathcal{L}\left(\frac{1-\ell_i}{d_i}, -\frac{1+\ell_i}{d_i}\right)$ , for any  $i = 1, \dots, N$ .

See Appendix A for the proof of Theorem 2.6. Our proof is by exhaustion, in that we show that the constraints provided by the assumptions of Theorem 2.6 restrict the allowed options to cases (i) and (ii).

**REMARK 2.7.** Assuming that  $g_1, \dots, g_N : \mathbb{R} \rightarrow \mathbb{R}$  are affine is not restrictive. Lemma 2.4 ensures that if  $g_i : \mathbb{R} \rightarrow \mathbb{R}$  is piecewise  $C^1$  and Lipschitz as  $\sigma_i$ , and  $F$  has a Jacobian matrix which is orthogonal almost everywhere, then  $F_i(x) = g_i(x) + d_i A^\top \sigma_i(Bx + b)$  must be piecewise affine. Therefore, given that the partition  $\{\Omega_1, \dots, \Omega_N\}$  and the number of its elements  $N \in \mathbb{N}$  are arbitrary, we can think of having a fine enough partition such that on every set  $\Omega_i$  the function  $g_i$  is affine.

**REMARK 2.8.** The choice  $\ell_i = 0$  belongs to both cases (i) and (ii). This means that, if  $A = B$ , it is possible to have some regions where there is no skip-connection, i.e.  $\ell_i = 0$ , and others where there is, i.e.,  $\ell_i \neq 0$ .

We remark that when we add a scalar to a vector, as in  $\ell_i x + c_i$ , we use a more compact notation for  $\ell_i x + c_i 1_n$ . It is also clear that maps of the form  $F_{i, v_i}(x) = F_i(x) + v_i$ , with  $v_i \in \mathbb{R}^n$  and  $F_i$  as in Theorem 2.6, still have an orthogonal Jacobian. Furthermore, since the product of orthogonal matrices is orthogonal, one could get networks with Jacobians that are orthogonal for almost every  $x$  by composing the above layers with global isometries, i.e., maps of the form  $x \mapsto Rx + b$  with  $R^\top R = RR^\top = I_n$  and  $b \in \mathbb{R}^n$ . This operation also allows to encode a generalisation of the residual layers of case (ii), as formalised in the next corollary.

**COROLLARY 2.9** (Corollary to Theorem 2.6). *Let  $N \in \mathbb{N}$  and  $\{\Omega_1, \dots, \Omega_N\}$  in  $\mathcal{P}(\mathbb{R}^n)$  be arbitrary. Consider  $G : \mathbb{R}^n \rightarrow \mathbb{R}^n$  defined as*

$$G(x) = \sum_{i=1}^N 1_{\Omega_i}(x) (\ell_i O x + c_i + d_i A^\top \sigma_i(Bx + b)),$$

$\sigma_i : \mathbb{R} \rightarrow \mathbb{R}$  Lipschitz continuous and piecewise  $C^1$ ,  $c_i, d_i \in \mathbb{R}$ ,  $\ell_i \in \mathbb{R} \setminus \{0\}$ , for every  $i = 1, \dots, N$ , and  $A, B, O \in \mathcal{O}(n)$ . Then,  $G'(x)$  is orthogonal for almost every  $x \in \mathbb{R}^n$  if and only if  $\sigma_i \in \mathcal{L}\left(\frac{1-\ell_i}{d_i}, -\frac{1+\ell_i}{d_i}\right)$  and  $A = BO^\top$ , i.e., if and only if  $G(x) = OF(x)$  with  $F$  as in case (ii).

We prove this result in Appendix B.

To conclude the section, let us introduce the following generalised notion of orthogonality.

**DEFINITION 2.10.** Let  $A \in \mathbb{R}^{n \times n}$ . We say that  $A$  is partially orthogonal, or equivalently that induces a partial isometry, writing  $A \in \mathcal{O}(n)$ , if  $\ker(A)^\perp \ni v \mapsto Av$  is an isometry.

This property can be intended as a natural weakening of the orthogonality condition, see [16], which here needs to be satisfied only on subspaces instead of the whole space. More explicitly, when  $A$  is non-singular, we recover the conventional notion of isometry.

As a direct consequence of the above definition, it holds that  $\mathcal{O}(n) \subset \mathcal{O}(n)$ . Moreover,  $A \in \mathcal{O}(n)$  if and only if the matrix  $AA^\top$  is a projection.

We conjecture that this condition, when applied to the almost-everywhere well-defined Jacobian matrix of a model, is enough to achieve trainability. Moreover, we claim that the dynamical isometry principle can be generalised to this regime, keeping the Jacobian close to being a partial-isometry as it is at initialisation. We will support these claims with numerical experiments in Section 5.

### 3 Networks with orthogonal Jacobian

We now point out some particular types of maps arising from (2.1), with the constraints given by Theorem 2.6. These maps are network layers with an orthogonal Jacobian almost everywhere. By the chain rule, the Jacobian matrix of the network  $\mathcal{N}_\theta = F_{\theta_L} \circ \dots \circ F_{\theta_1}$ , when well defined, takes the form  $\mathcal{N}'_\theta(x) = F'_{\theta_L}(y_{L-1}) \cdot F'_{\theta_{L-1}}(y_{L-2}) \cdot \dots \cdot F'_{\theta_1}(x)$ , where  $y_0 = x$  and  $y_i = F_{\theta_i}(y_{i-1})$ , and is orthogonal.

The first two types of layers that we describe are efficient to implement, and we test them in the numerical experiments in Section 5. The third example is presented to show the possibility of designing less conventional layers which still ensure the correct orthogonality constraint on their Jacobian.

**Modified ResNet layer** The first choice is given by

$$F(x) = x - 2B^\top \text{ReLU}_k(Bx + b), \quad (3.1)$$

where, setting  $x_1 < x_2 < \dots < x_k$ ,

$$\text{ReLU}_k(x) = \sum_{i=1}^k (-1)^{i-1} \text{ReLU}(x - x_i), \quad (3.2)$$

is a piecewise affine Lipschitz-continuous function with slopes either 0 or 1, i.e.,  $\text{ReLU}_k \in \mathcal{L}(0, 1)$ . The case  $k = 1$  with  $x_1 = 0$  coincides with the usual  $\text{ReLU}(x) = \max\{0, x\}$ . The case  $k = 2$  allows to represent the activation HardTanh. We include the plot of  $\text{ReLU}_3$ , with  $x_1 = -1$ ,  $x_2 = 0$ , and  $x_3 = 1.5$ , in Figure 1a. The  $F$  in (3.1) corresponds to case (ii) with  $N = 1$ ,  $l_1 = 1$ ,  $c_1 = 0$ , and  $d_1 = -2$  so that

$$\frac{1 - l_1}{d_1} = 0, \quad -\frac{1 + l_1}{d_1} = 1.$$

We further discuss this example in the experimental section, comparing the case  $k = 1$ , which is a well-known layer corresponding to the explicit Euler step along the negative gradient of the convex potential  $V(x) = 1^\top \gamma(Bx + b)$ ,  $\gamma(s) = \max\{0, s\}^2/2$ , and the case  $k = 3$ . The layer with  $k = 1$  has been used in [31, 38, 41, 33] to get 1-Lipschitz networks. We also remark that considering  $d = 1$  in (3.1), we would get Jacobians which are partially orthogonal, as proven in Appendix F, and the models are still trainable as we show in Section 5.

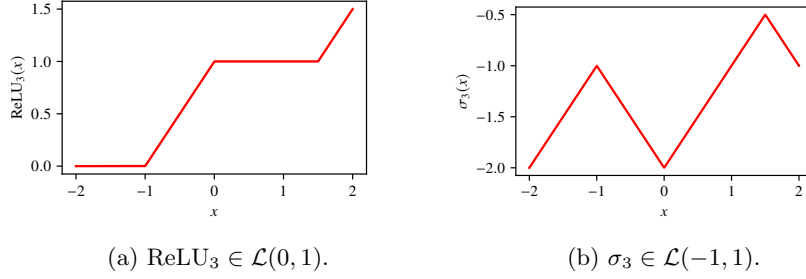


Figure 1: Plot of two piecewise affine Lipschitz continuous scalar functions.

**Modified feedforward network** Another relevant example corresponds to the case without skip connection, i.e.,  $g(x) = 0$ . Fixing  $N = 1$  and  $d_1 = 1$ , in (i), and choosing  $\sigma(x) = |x|$ , we recover the layer  $F(x) = A^\top |Bx + b|$ , where  $|Bx + b| \in \mathbb{R}^n$  has  $i$ -th entry defined as  $|Bx + b|_i = |(Bx + b)_i|$ . Similarly to the generalisation of ReLU to  $\text{ReLU}_k$  done above, we could also consider a more generic activation in  $\mathcal{L}(-1, 1)$ . We write it as

$$\sigma_k(x) = x - 2\text{ReLU}_k(x), \quad (3.3)$$

with  $\text{ReLU}_k$  defined as in (3.2). We plot in Figure 1b the function  $\sigma_3$  with the same choices for  $x_1, x_2, x_3$  as for  $\text{ReLU}_3$ . The lack of monotonicity makes  $\sigma_k$  an unconventional activation function. Still, this property allows it to generate nonlinear layers for a feedforward network with  $\|F'(x)\|_2 = 1$  almost everywhere, which would not be possible for monotonic 1-Lipschitz activations, as proven in [1, Theorem 1]. We further emphasize that substituting  $\sigma_k$  with  $\text{ReLU}_k$  leads to partial orthogonal layers, see Appendix F.

The two examples considered above are globally continuous, trainable and have a Lipschitz constant bounded by 1, making them relevant to applications in inverse problems, generative modelling, and adversarial robustness.

**Alternative skip connection** The framework we derived in the previous section also allows us to recover modified residual networks where the conventional identity skip-connection is replaced. We now provide an example to illustrate the wider range of possibilities. Let  $\Omega_1 = \{x \in \mathbb{R}^n : a^\top x < 0\}$  and  $\Omega_2 = \{x \in \mathbb{R}^n : a^\top x > 0\}$ , where  $a \in \mathbb{R}^n$  could be a learnable vector. We then define the skip-connections as

$$g(x) = -1_{\Omega_1}(x)x + 1_{\Omega_2}(x)x,$$

meaning that  $l_1 = -1$ ,  $l_2 = 1$ , and  $c_1 = c_2 = 0$ . A compatible choice of activation functions leads to

$$\rho(x) = 2(1_{\Omega_1}(x)\text{ReLU}_k(x) - 1_{\Omega_2}(x)\text{ReLU}_k(x)),$$

where  $k \in \mathbb{N}$ , and we have fixed  $d_1 = d_2 = 1$  for simplicity. We thus obtain the network layer

$$F(x) = g(x) + B^\top \rho(Bx + b) = 1_{\Omega_1}(x)(-x + 2B^\top \text{ReLU}_k(Bx + b)) + 1_{\Omega_2}(x)(x - 2B^\top \text{ReLU}_k(Bx + b)).$$

Setting  $s(x) = \text{sign}(a^\top x)$ , we can rewrite the above layer as

$$F(x) = s(x)(x - 2B^\top \text{ReLU}_k(Bx + b)),$$

where  $\text{ReLU}_k$  is defined as in (3.2) for a suitable choice of breaking points  $x_1, \dots, x_k$ . The resulting map, up to a sign change, is the same vector field we constructed in (3.1), however, in this case it is not globally continuous. We point out that  $s(x)$  can be interpreted as a gating mechanism, similar to those in Highway Networks [43] or in LTSMs [21].

## 4 Limit models and dynamical isometry

The theory we developed in Section 2 is independent on the underlying partition  $\{\Omega_1, \dots, \Omega_N\}$  we choose, but we instead focus on the selection of  $N$ , and the scalars  $\{(l_i, c_i) \mid i = 1, \dots, N\}$ . In this section, we aim to reverse this perspective and investigate the role of the chosen partition.

Let  $\Omega \subset \mathbb{R}^n$  be a compact and connected set, and consider a finite collection of subsets  $\{\Omega_i\}_{i \in [1, N]} \in \mathcal{P}(\Omega)$ . Then, setting  $d_1 = \dots = d_N = 1$ , any  $F$  in the form described by case (ii) can be rewritten as

$$\mathcal{F}_\Omega(x; \tilde{m}, \tilde{q}) := \tilde{m}(x)x + \tilde{q}(x) + 1_\Omega(x)B^\top \sigma(Bx + b; \tilde{\mu}_1(x), \tilde{\mu}_2(x)), \quad (4.1)$$

where

$$\begin{aligned} \tilde{\mu}_1(x) &:= 1 - \tilde{m}(x), \quad \tilde{\mu}_2(x) := -1 - \tilde{m}(x), \\ \tilde{m}(x) &= \sum_{i=1}^N 1_{\Omega_i}(x)\ell_i, \quad \tilde{q}(x) = \sum_{i=1}^N 1_{\Omega_i}(x)c_i. \end{aligned}$$

The primary advantage of this new formulation is that it embeds the underlying partition within the piecewise-constant functions  $\tilde{m}$  and  $\tilde{q}$ . This shift allows us to focus directly on the behaviour of these functions.

Let us consider then two sequences  $\{\tilde{m}_i\}_{i \in \mathbb{N}}$  and  $\{\tilde{q}_i\}_{i \in \mathbb{N}}$  of piecewise constant functions converging to two continuous functions  $m : \Omega \rightarrow \mathbb{R}$  and  $q : \Omega \rightarrow \mathbb{R}$ , respectively. Then, the natural question that arises is how to characterise the limiting architecture defined by these sequences. We (partially) answer the above question with the following density result.

**THEOREM 4.1.** *Let us consider a compact and connected set  $\Omega \subset \mathbb{R}^n$ ,  $B \in \mathcal{O}(n)$ ,  $b \in \mathbb{R}^n$ , and  $\varepsilon > 0$ . Then, for any pair of continuous functions  $m, q : \Omega \rightarrow \mathbb{R}$ , there exists  $N \in \mathbb{N}$ , a finite collection of subsets  $\{\Omega_i\}_{i \in [1, N]} \in \mathcal{P}(\Omega)$ , and  $2N$  scalars  $m_1, \dots, m_N, q_1, \dots, q_N \in \mathbb{R}$  such that*

$$\max_{x \in \Omega} \|\mathcal{F}_\Omega(x; m, q) - \mathcal{F}_\Omega(x; \tilde{m}, \tilde{q})\|_\infty < \varepsilon,$$

where  $\mathcal{F}_\Omega(x; \cdot, \cdot)$  is given by (4.1) and

$$\tilde{m}(x) = \sum_{i=1}^N 1_{\Omega_i}(x)m_i, \quad \tilde{q}(x) = \sum_{i=1}^N 1_{\Omega_i}(x)q_i.$$

We now prove it for  $\sigma(x; \alpha, \beta) = \max\{\alpha x, \beta x\}$ ,  $\alpha, \beta \in \mathbb{R}$ . For the general proof see Appendix C.

*Proof.* The two considered functions are of the form

$$\begin{aligned} \mathcal{F}_\Omega(x; m, q) &= m(x)x + q(x) + B^\top \max\{\mu_1(x)(Bx + b), \mu_2(x)(Bx + b)\}, \\ \mathcal{F}_\Omega(x; \tilde{m}, \tilde{q}) &= \tilde{m}(x)x + \tilde{q}(x) + B^\top \max\{\tilde{\mu}_1(x)(Bx + b), \tilde{\mu}_2(x)(Bx + b)\}. \end{aligned} \quad (4.2)$$

Since  $\max\{u, v\} = u + \text{ReLU}(v - u)$ ,  $u, v \in \mathbb{R}$ , we write

$$\max\{\mu_1(x)(Bx + b), \mu_2(x)(Bx + b)\} = (1 - m(x))(Bx + b) + 2\text{ReLU}(-(Bx + b)). \quad (4.3)$$

Then, substituting back in (4.1), we obtain that

$$\begin{aligned} \|\mathcal{F}_\Omega(x; m, q) - \mathcal{F}_\Omega(x; \tilde{m}, \tilde{q})\|_\infty &= \|q(x) - \tilde{q}(x) + (m(x) - \tilde{m}(x))x \\ &\quad + (1 - m(x))(x + B^\top b) - (1 - \tilde{m}(x))(x + B^\top b)\|_\infty \\ &\leq |q(x) - \tilde{q}(x)| + |\tilde{m}(x) - m(x)|\|b\|_2. \end{aligned}$$

The density of piecewise-constant functions in continuous ones on compact sets allows us to conclude.  $\square$

The above Theorem opens up to a much broader class of network layers presenting non-affine skip connections that can be approximated arbitrarily well by choosing a fine enough partition  $\{\Omega_1, \dots, \Omega_N\}$  in  $\mathcal{P}(\Omega)$ . Furthermore, based on the density results provided by Theorem 4.1, we conjecture that the limit layers  $\mathcal{F}_\Omega(x; m, q)$  inherit the good trainability properties from  $\mathcal{F}_\Omega(x; \tilde{m}, \tilde{q})$ . We will numerically support this claim in the numerical experiments, see Section 5.

To conclude, following up on this same idea, let us restrict our attention to the case  $\sigma(x; \alpha, \beta) = \max\{\alpha x, \beta x\}$ , with  $\alpha, \beta \in \mathbb{R}$ . Despite generally  $x \mapsto \mathcal{F}_\Omega(x; m, q)$  does not have an orthogonal Jacobian, recalling (4.3) and defining  $B' = -B \in \mathcal{O}(n)$  and  $b' = -b$ , we get

$$\begin{aligned} \mathcal{F}_\Omega(x; m, q) &= m(x)x + q(x) + (1 - m(x))(x + B^\top b) + 2B^\top \text{ReLU}(-Bx - b) \\ &= q(x) + (1 - m(x))(B')^\top b' + (x - 2(B')^\top \text{ReLU}(B'x + b')) \end{aligned} \quad (4.4)$$

that provides a generalisation of (3.1) , which is known to have an orthogonal Jacobian matrix almost everywhere. This argument suggests that maps of the form (4.4) with  $m, q : \Omega \rightarrow \mathbb{R}$  continuous functions, are potentially more expressive than maps of the type  $x \mapsto x - 2(B')^\top \text{ReLU}(B'x + b')$  while preserving their trainability properties. We can further improve the trainability through the following theorem.

**THEOREM 4.2.** *Consider a convex and connected set  $\Omega \subset \mathbb{R}^n$ , a vector  $b \in \mathbb{R}^n$ , and two Lipschitz continuous functions  $m, q : \Omega \rightarrow \mathbb{R}$  with Lipschitz constants  $\text{Lip}(m)$  and  $\text{Lip}(q)$ . Let  $\varepsilon > 0$  be such that*

$$\text{Lip}(m)\|b\|_2 \leq \frac{\varepsilon}{2}, \text{ and } \text{Lip}(q) \leq \frac{\varepsilon}{2\sqrt{n}}$$

for almost every  $x \in \Omega$ . Then, all the singular values of the Jacobian of  $f(x) = \mathcal{F}_\Omega(x; m, q)$ , when it is well defined, belong to the interval  $[1 - \varepsilon, 1 + \varepsilon]$ .

The dynamical isometry principle requires the network Jacobian to have singular values around 1. Thus, Theorem 4.2 provides a practical way to promote this property over these limiting networks by selecting functions  $m, q : \Omega \rightarrow \mathbb{R}$  with a moderate Lipschitz constant, and regularising for  $\|b\|_2$  to be small. Moreover, applying this to every layer allows the entire network to satisfy an analogous estimate.

*Proof.* Since  $q$  and  $m$  are Lipschitz continuous, they are also differentiable almost everywhere by Rademacher's Theorem [11, Theorem 3.1.6]. Hence, for almost every  $x \in \mathbb{R}^n$ , we can compute the Jacobian of  $f$  as

$$f'(x) = 1_n \nabla q(x)^\top - B^\top b \nabla m(x)^\top + (I_n - 2B^\top D(x)B),$$

where  $D(x) = \text{diag}(\text{ReLU}'(Bx + b)) \in \{D = \text{diag}(d_1, \dots, d_n) \mid d_1, \dots, d_n \in \{0, 1\}\}$ . We know that  $I_n - 2B^\top D(x)B$  is orthogonal, so  $f'(x)$  is a rank-two perturbation of an orthogonal matrix. When  $m$  and  $q$  are constant,  $f'(x)$  is orthogonal as known from Theorem 2.6.

By Weyl's inequality for singular values, see [22, Corollary 7.3.5], we get that the  $i$ -th singular value of  $f'(x)$ , i.e.,  $\sigma_i(f'(x))$ , satisfies

$$\begin{aligned} |\sigma_i(f'(x)) - 1| &\leq \|1_n \nabla q(x)^\top - B^\top b \nabla m(x)^\top\|_2 \\ &\leq \|b\|_2 \|\nabla m(x)\|_2 + \sqrt{n} \|\nabla q(x)\|_2 \\ &\leq \text{Lip}(m)\|b\|_2 + \sqrt{n} \text{Lip}(q) \leq \varepsilon. \end{aligned}$$

We conclude that, for any  $i \in \{1, \dots, n\}$  and almost any  $x \in \Omega$ ,  $\sigma_i(f'(x)) \in [1 - \varepsilon, 1 + \varepsilon]$  holds true.  $\square$

We remark that the reasoning in Theorem 4.2 could be repeated on each set of a partition  $\{\Omega_1, \dots, \Omega_N\}$  in  $\mathcal{P}(\Omega)$ , where we would recover the exact orthogonality for  $m = \tilde{m}$  and  $q = \tilde{q}$  constant on each subset  $\Omega_i$  for the partition.

## 5 Numerical experiments

We focus on classifying the images of the Fashion MNIST dataset and train models with a varying number of layers  $L \in \{10, 50, 200\}$ . Appendix D provides a more detailed description of the experimental setup. The aim of these experiments is not to achieve state-of-the-art performance with the selected architectures, but to support our theoretical results showing that enforcing Jacobian orthogonality is sufficient to enable deep networks to converge to a reasonable accuracy comparable to that of previously studied architectures. Our source code will be published upon acceptance. We conduct the following three blocks of experiments.

**First block.** We first investigate models characterised by Theorem 2.6. As representatives of case (i), we choose  $x \mapsto A^\top \rho(Bx + b)$  with  $\rho \in \{\sigma_1, \sigma_3\}$  and, to represent case (ii), we pick  $x \mapsto x - B^\top \rho(Bx + b)$  where  $\rho \in \{2\text{ReLU}, 2\text{ReLU}_3\}$ . The nodes in  $\text{ReLU}_3$  and  $\sigma_3$  are set to  $\{-1, 0, 1\}$  for both models. We compare the performance with a ResNet with layers  $x \mapsto x + 2A^\top \text{ReLU}(Bx + b)$ ,  $A, B \in \mathcal{O}(n)$ , denoted as  $\text{ResNet}_{A, B}$ . The convolutional filters are initialised as Dirac tensors, i.e., identity maps, and are of shape  $F \times F \times C \times C$ , with  $F = 3$  the size of the convolutional filters, and  $C = 8$  the number of channels.

**Second block.** These experiments support the claims on the partial orthogonality we made at the end of Section 2. We consider a model as in case (i) and one as in case (ii), both with ReLU as activation. Moreover, we also analyse a third model based on case (i) with  $\sigma(x) = \text{LeakyReLU}(x) = \max\{0.3x, x\}$ . We show in Appendix F that the first two models have Jacobians which, when well defined, are partially orthogonal, whereas the third model’s Jacobian is close to being partially orthogonal.

**Third block.** As remarked in Section 4, the elements in the closure of the set of networks with orthogonal Jacobian do not generally satisfy this constraint. However, the closeness to the orthogonal layers shown in Theorem 4.1, and the control on the singular values of the Jacobian proposed in Theorem 4.2, motivates the investigation of these architectures. We use layers of the form (4.4) with  $q(x) = 0$  for all  $x \in \mathbb{R}^{n \times n}$ , and test three choices of  $m : \mathbb{R}^{n \times n} \rightarrow \mathbb{R}$ :

- i.  $m_1(x) = 1$ , which is our baseline and gives layers of the form  $x \mapsto x - 2B^\top \text{ReLU}(Bx + b)$ ,
- ii.  $m_2(x) = \exp(-\|x\|_F^2)/100$ , where  $\|\cdot\|_F$  is the Frobenius norm, and we have  $\|\nabla m_2(x)\|_F \in [0, e^{-1/2}\sqrt{2}/100]$ ,
- iii.  $m_3(x) = W_1 * \text{ReLU}(W_2 * x + w_3)$ , with  $*$  the convolution product and  $W_1 \in \mathbb{R}^{1 \times 1 \times C \times 1}$ ,  $W_2 \in \mathbb{R}^{n \times n \times C \times C}$ ,  $w_3 \in \mathbb{R}^{1 \times 1 \times C}$  trainable weights, with  $x \in \mathbb{R}^{n \times n \times C}$ .

The weights in  $m_3$  are initialised from a normal distribution. Here, as activation function, we use  $\sigma(x) = 2\text{ReLU}(x)$ .

## 5.1 Results

### 5.1.1 Piecewise affine models based on Theorem 2.6

Table 1 shows that all proposed models demonstrate a validation accuracy at least comparable to the baseline architecture. ResNet<sub>A,B</sub> stops training with 50 and 200 layers, whereas ours do not suffer in those regimes. The networks using  $\sigma_1$  and  $\sigma_3$ , which are feedforward networks, perform comparably to ResNets. These outcomes strongly support our theory.

Table 1: Piecewise affine models. The table reports the classification accuracy on the validation set of Fashion MNIST. We test models with  $L$  layers,  $L \in \{10, 50, 200\}$ , and regularisation parameter  $\alpha \in \{0, 0.001\}$ .  $\alpha = 0$  corresponds to orthogonal initialisation with no regularisation.

Model	$\alpha$	10	50	200
ResNet <sub>A,B</sub>	0	89.2%	8.7%	10.0%
	0.001	88.1%	11.1%	10.0%
FF- $\sigma_1$	0	86.8%	87.1%	86.0%
	0.001	87.0%	86.5%	86.7%
FF- $\sigma_3$	0	89.3%	83.7%	84.3%
	0.001	90.6%	83.9%	83.8%
ResNet-ReLU	0	87.2%	88.8%	88.2%
	0.001	88.8%	90.1%	88.3%
ResNet-ReLU <sub>3</sub>	0	89.7%	87.8%	89.1%
	0.001	89.6%	88.8%	87.2%

### 5.1.2 Partial Orthogonal Models

As reported in Figure 2, we observe a convergent training for all the considered models independently of the number of layers. These results corroborate our conjecture that a.e. partial orthogonality instead of a.e. orthogonality of the Jacobian may be sufficient to retain the training properties. Still, this conjecture needs more theoretical and experimental validation.

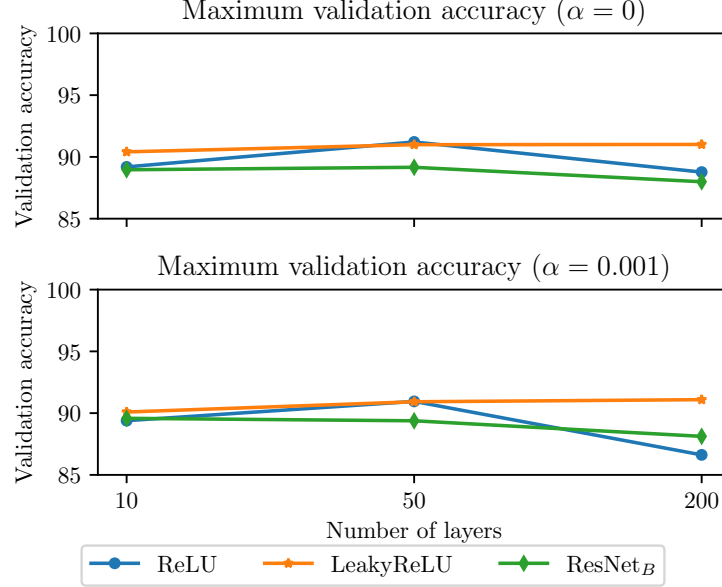


Figure 2: Models with partial orthogonality. We compare two feedforward networks as in case (i), with activations ReLU and LeakyReLU, plus a ResNet of layers  $x \mapsto x - B^\top \text{ReLU}(Bx + b) =: \text{ResNet}_B(x)$ ,  $B \in \mathcal{O}(n)$ . The top plot refers to the case without regularisation, i.e.,  $\alpha = 0$ , while the other to the case with it, i.e.,  $\alpha = 0.001$ .

### 5.1.3 Limit models based on Theorem 4.1

In Table 2, we show that the limiting models with  $m_2$  and  $m_3$ , which we recall are not piecewise affine, present performances comparable to  $m_1$ , which is known to have an orthogonal Jacobian matrix almost everywhere. It is worth pointing out that  $m_2$  satisfies the hypotheses of Theorem 4.2, having a moderate derivative, whereas  $m_3$  is randomly initialised. Since no regularisation is used to limit the growth of its weight norms, the ability to train appears to be deeply connected with their closeness to architectures with orthogonal Jacobian. These experiments suggest that characterising more general types of network layers well approximated by maps with an orthogonal Jacobian is a promising direction for the future.

Table 2: Limit models. The table reports the classification accuracy on the validation set of Fashion MNIST. We test models with  $L$  layers,  $L \in \{10, 50, 200\}$ , and regularisation parameter  $\alpha \in \{0, 0.001\}$ .  $\alpha = 0$  corresponds to orthogonal initialisation with no regularisation. The first column indicates the function  $m$  in Theorem 4.1, whereas  $q = 0$ . For  $m_3$ , we report the averages of two experiments, and the term after  $\pm$  gives the interval where the results belong.

Model	$\alpha$	10	50	200
$m_1$	0	87.2%	88.8%	88.2%
	0.001	88.8%	90.1%	88.3%
$m_2$	0	89.5%	89.4%	88.6%
	0.001	89.4%	88.9%	89.8%
$m_3$	0	89.6 $\pm$ 0.2%	88.5 $\pm$ 0.4%	87.9 $\pm$ 0.1%
	0.001	87.7 $\pm$ 0.1%	88.0 $\pm$ 0.6%	88.2 $\pm$ 0.1%

### 5.1.4 Regularisation

Comparing the results in Table 1, Figure 2 and Table 2 for the different values of  $\alpha$ , we see that the regularisation terms play a rather marginal role. This is furthermore emphasized looking at the performance

change compared with the substantial increase in training time required to compute the additional terms (see Appendix E).

## 6 Summary and discussion

In this paper, we presented a general characterisation of a class of network layers with an orthogonal Jacobian matrix almost everywhere. From this general form, we deduced specific, practically implementable layers that directly generalise known architectures. In addition, we derived a more general class of layers, not necessarily with an orthogonal Jacobian, that are approximated arbitrarily well by our architectures, and we showed numerically that these approximations inherit the desirable trainability properties associated with orthogonal Jacobians. We then empirically demonstrated the effectiveness of Jacobian orthogonality as a technique to make very deep networks trainable.

Our theoretical and empirical results open the way to several extensions. The experiments with partially orthogonal Jacobians indicate that the strict orthogonality requirements might be relaxed without compromising trainability. Similarly, the promising performance of the limiting nonlinear networks highlights the potential value of further analysing skip connections in relation to the data and task.

## References

- [1] Cem Anil, James Lucas, and Roger Grosse. Sorting out Lipschitz function approximation. In *International Conference on Machine Learning*, pages 291–301. PMLR, 2019.
- [2] Jimmy Lei Ba, Jamie Ryan Kiros, and Geoffrey E Hinton. Layer Normalization. *arXiv preprint arXiv:1607.06450*, 2016.
- [3] Yoshua Bengio, Patrice Simard, and Paolo Frasconi. Learning long-term dependencies with gradient descent is difficult. *IEEE Transactions on Neural Networks*, 5(2):157–166, 1994.
- [4] Pakshal Bohra, Joaquim Campos, Harshit Gupta, Shayan Aziznejad, and Michael Unser. Learning Activation Functions in Deep (Spline) Neural Networks. *IEEE Open Journal of Signal Processing*, 1:295–309, 2020.
- [5] Alexandre Caboussat, Roland Glowinski, Dimitrios Gourzoulidis, and Marco Picasso. Numerical Approximation Of Orthogonal Maps. *SIAM Journal on Scientific Computing*, 2019.
- [6] Antonin Chambolle, Alessandro Giacomini, and Marcello Ponsiglione. Piecewise rigidity. *Journal of Functional Analysis*, 244(1):134–153, 2007.
- [7] Sergio Conti and Francesco Maggi. Confining Thin Elastic Sheets and Folding Paper. *Archive for Rational Mechanics and Analysis*, 187:1–48, 2008.
- [8] Bernard Dacorogna, Paolo Marcellini, and Emanuele Paolini. Lipschitz-continuous local isometric immersions: rigid maps and origami. *Journal de Mathématiques Pures et Appliquées*, 90(1):66–81, 2008.
- [9] Bernard Dacorogna, Paolo Marcellini, and Emanuele Paolini. Functions with Orthogonal Hessian. *Differential and Integral Equations*, 23, 08 2010.
- [10] Francesco Della Santa and Sandra Pieraccini. Discontinuous neural networks and discontinuity learning. *Journal of Computational and Applied Mathematics*, 419:114678, 2023.
- [11] Herbert Federer. *Geometric Measure Theory*. Springer, 2014.
- [12] Clara Lucía Galimberti, Luca Furieri, Liang Xu, and Giancarlo Ferrari-Trecate. Hamiltonian Deep Neural Networks Guaranteeing Non-vanishing Gradients by Design. *IEEE Transactions on Automatic Control*, 68(5):3155–3162, 2023.
- [13] Xavier Glorot and Yoshua Bengio. Understanding the difficulty of training deep feedforward neural networks. In *Proceedings of the Thirteenth International Conference on Artificial Intelligence and Statistics*, pages 249–256. JMLR Workshop and Conference Proceedings, 2010.
- [14] Ishaan Gulrajani, Faruk Ahmed, Martin Arjovsky, Vincent Dumoulin, and Aaron C Courville. Improved Training of Wasserstein GANs. *Advances in Neural Information Processing Systems*, 30, 2017.
- [15] Eldad Haber and Lars Ruthotto. Stable Architectures for Deep Neural Networks. *Inverse Problems*, 34(1):014004, 2017.

[16] Paul R Halmos and Jack E McLaughlin. Partial isometries. 1963.

[17] Kaiming He, Xiangyu Zhang, Shaoqing Ren, and Jian Sun. Delving Deep into Rectifiers: Surpassing Human-Level Performance on ImageNet Classification. In *Proceedings of the IEEE International Conference on Computer Vision*, pages 1026–1034, 2015.

[18] Kaiming He, Xiangyu Zhang, Shaoqing Ren, and Jian Sun. Deep Residual Learning for Image Recognition. In *Proceedings of the IEEE Conference on Computer Vision and Pattern Recognition*, pages 770–778, 2016.

[19] Johannes Hertrich, Sebastian Neumayer, and Gabriele Steidl. Convolutional Proximal Neural Networks and Plug-and-Play Algorithms. *Linear Algebra and its Applications*, 631:203–234, 2021.

[20] Sepp Hochreiter, Yoshua Bengio, Paolo Frasconi, and Jürgen Schmidhuber. Gradient Flow in Recurrent Nets: The Difficulty of Learning Long-Term Dependencies. In *A Field Guide to Dynamical Recurrent Networks*, pages 237–243. 2001.

[21] Sepp Hochreiter and Jürgen Schmidhuber. Long Short-Term Memory. *Neural Computation*, 9(8):1735–1780, 1997.

[22] Roger A Horn and Charles R Johnson. *Matrix Analysis*. Cambridge University Press, 2012.

[23] Sergey Ioffe and Christian Szegedy. Batch Normalization: Accelerating Deep Network Training by Reducing Internal Covariate Shift. In *International Conference on Machine Learning*, pages 448–456. PMLR, 2015.

[24] Xiaojie Jin, Chunyan Xu, Jiashi Feng, Yunchao Wei, Junjun Xiong, and Shuicheng Yan. Deep Learning with S-shaped Rectified Linear Activation Units. In *Proceedings of the AAAI Conference on Artificial Intelligence*, volume 30, 2016.

[25] Bernd Kirchheim. Rigidity and Geometry of Microstructures. Lecture Notes 16, Max Planck Institut, Leipzig, 2003.

[26] Günter Klambauer, Thomas Unterthiner, Andreas Mayr, and Sepp Hochreiter. Self-Normalizing Neural Networks. *Advances in Neural Information Processing Systems*, 30, 2017.

[27] Insung Kong, Juntong Chen, Sophie Langer, and Johannes Schmidt-Hieber. On the expressivity of deep Heaviside networks. *arXiv preprint arXiv:2505.00110*, 2025.

[28] Sebastian Lunz, Ozan Öktem, and Carola-Bibiane Schönlieb. Adversarial Regularizers in Inverse Problems. *Advances in Neural Information Processing Systems*, 31, 2018.

[29] Andrew L Maas, Awni Y Hannun, Andrew Y Ng, et al. Rectifier Nonlinearities Improve Neural Network Acoustic Models. In *Proceedings of the 30th International Conference on Machine Learning*, volume 30, page 3. Atlanta, GA, 2013.

[30] Sofya Maslovskaya and Sina Ober-Blöbaum. Symplectic Methods in Deep Learning. *IFAC-PapersOnLine*, 58(17):85–90, 2024.

[31] Laurent Meunier, Blaise J Delattre, Alexandre Araujo, and Alexandre Allauzen. A Dynamical System Perspective for Lipschitz Neural Networks. In *International Conference on Machine Learning*, pages 15484–15500. PMLR, 2022.

[32] Takeru Miyato, Toshiki Kataoka, Masanori Koyama, and Yuichi Yoshida. Spectral Normalization for Generative Adversarial Networks. *arXiv preprint arXiv:1802.05957*, 2018.

[33] Davide Murari, Takashi Furuya, and Carola-Bibiane Schönlieb. Approximation theory for 1-Lipschitz Resnets. *arXiv preprint arXiv:2505.12003*, 2025.

[34] Sergei Ovchinnikov. Max-Min Representation of Piecewise Linear Functions. *arXiv preprint math/0009026*, 2000.

[35] Razvan Pascanu, Tomas Mikolov, and Yoshua Bengio. On the difficulty of training Recurrent Neural Networks. In *International Conference on Machine Learning*, pages 1310–1318. PMLR, 2013.

[36] Jeffrey Pennington, Samuel Schoenholz, and Surya Ganguli. Resurrecting the sigmoid in deep learning through dynamical isometry: theory and practice. *Advances in Neural Information Processing Systems*, 30, 2017.

[37] Tomaso Poggio, Hrushikesh Mhaskar, Lorenzo Rosasco, Brando Miranda, and Qianli Liao. Why and When Can Deep – but Not Shallow – Networks Avoid the Curse of Dimensionality: a Review. *International Journal of Automation and Computing*, 14(5):503–519, 2017.

- [38] Bernd Prach, Fabio Brau, Giorgio Buttazzo, and Christoph H Lampert. 1-Lipschitz Layers Compared: Memory, Speed, and Certifiable Robustness. In *Proceedings of the IEEE/CVF Conference on Computer Vision and Pattern Recognition*, pages 24574–24583, 2024.
- [39] Ernest Ryu, Jialin Liu, Sicheng Wang, Xiaohan Chen, Zhangyang Wang, and Wotao Yin. Plug-and-Play Methods Provably Converge with Properly Trained Denoisers. In *International Conference on Machine Learning*, pages 5546–5557. PMLR, 2019.
- [40] Andrew M Saxe, James L McClelland, and Surya Ganguli. Exact solutions to the nonlinear dynamics of learning in deep linear neural networks. *arXiv preprint arXiv:1312.6120*, 2013.
- [41] Ferdia Sherry, Elena Celledoni, Matthias J Ehrhardt, Davide Murari, Brynjulf Owren, and Carola-Bibiane Schönlieb. Designing Stable Neural Networks using Convex Analysis and ODEs. *Physica D: Nonlinear Phenomena*, 463:134159, 2024.
- [42] Sahil Singla and Soheil Feizi. Skew Orthogonal Convolutions. In *International Conference on Machine Learning*, pages 9756–9766. PMLR, 2021.
- [43] Rupesh Kumar Srivastava, Klaus Greff, and Jürgen Schmidhuber. Highway Networks. *arXiv preprint arXiv:1505.00387*, 2015.
- [44] Asher Trockman and J Zico Kolter. Orthogonalizing Convolutional Layers with the Cayley Transform. *arXiv preprint arXiv:2104.07167*, 2021.
- [45] Yusuke Tsuzuku, Issei Sato, and Masashi Sugiyama. Lipschitz-Margin Training: Scalable Certification of Perturbation Invariance for Deep Neural Networks. *Advances in Neural Information Processing Systems*, 31, 2018.
- [46] Thomas Unterthiner and Sepp Hochreiter. Understanding Very Deep Networks via Volume Conservation. 2016.
- [47] Jiayun Wang, Yubei Chen, Rudrasis Chakraborty, and Stella X Yu. Orthogonal Convolutional Neural Networks. In *Proceedings of the IEEE/CVF Conference on Computer Vision and Pattern Recognition*, pages 11505–11515, 2020.
- [48] Yuxin Wu and Kaiming He. Group Normalization. In *Proceedings of the European Conference on Computer Vision (ECCV)*, pages 3–19, 2018.
- [49] Lechao Xiao, Yasaman Bahri, Jascha Sohl-Dickstein, Samuel Schoenholz, and Jeffrey Pennington. Dynamical Isometry and a Mean Field Theory of CNNs: How to Train 10,000-Layer Vanilla Convolutional Neural Networks. In *International Conference on Machine Learning*, pages 5393–5402. PMLR, 2018.
- [50] Bing Xu, Naiyan Wang, Tianqi Chen, and Mu Li. Empirical Evaluation of Rectified Activations in Convolutional Network. *arXiv preprint arXiv:1505.00853*, 2015.
- [51] Dmitry Yarotsky. Error bounds for approximations with deep ReLU networks. *Neural Networks*, 94:103–114, 2017.
- [52] Penghang Yin, Jiancheng Lyu, Shuai Zhang, Stanley J. Osher, Yingyong Qi, and Jack Xin. Understanding Straight-Through Estimator in Training Activation Quantized Neural Nets. In *International Conference on Learning Representations*, 2019.
- [53] Yucong Zhou, Zezhou Zhu, and Zhao Zhong. Learning specialized activation functions with the Piecewise Linear Unit. In *Proceedings of the IEEE/CVF International Conference on Computer Vision*, pages 12095–12104, 2021.

## Appendix

### A Proof of Theorem 2.6

In this appendix, we use the notation

$$\mathcal{D}(\alpha_1, \alpha_2) := \{D = \text{diag}(d_1, \dots, d_n) \in \mathbb{R}^{n \times n} : d_1, \dots, d_n \in \{\alpha_1, \alpha_2\}\},$$

with  $\alpha_1, \alpha_2 \in \mathbb{R}$ , to denote the set of diagonal matrices with entries in a set of two elements  $\{\alpha_1, \alpha_2\}$ .

Consider an arbitrary partition  $\{\Omega_1, \dots, \Omega_N\}$  in  $\mathcal{P}(\mathbb{R}^n)$ . To simplify the notation and keep track of the slopes, if  $\sigma_i \in \mathcal{L}(\alpha_i, \beta_i)$ , we write  $\sigma_i(x) = \sigma(x; \alpha_i, \beta_i)$ . When considering the derivative  $\sigma'_i(x)$ , we use the notation  $\sigma'(x; \alpha_i, \beta_i)$ . Furthermore, we denote with  $F'_{\Omega_i}(x) \in \mathbb{R}^{n \times n}$ ,  $i = 1, \dots, N$ , the Jacobian matrix of the restriction  $F_{\Omega_i} : \Omega_i \rightarrow \mathbb{R}^n$  of  $F$  to  $\Omega_i$ .

**Verification that (i) and (ii) have orthogonal Jacobians:** **Case (i):** Let  $x \in \Omega_i$ . We have

$$F_{\Omega_i}(x) = d_i A^\top \sigma \left( Bx + b; -\frac{1}{d_i}, \frac{1}{d_i} \right) + c_i$$

and hence

$$F'_{\Omega_i}(x) = d_i A^\top \text{diag} \left( \sigma' \left( Bx + b; -\frac{1}{d_i}, \frac{1}{d_i} \right) \right) B =: d_i A^\top D_i(x) B.$$

Because of the properties of  $\sigma$ , for almost every  $x \in \Omega_i$ ,  $D_i(x) \in \mathcal{D}(-1/d_i, 1/d_i)$ . We conclude

$$F'_{\Omega_i}(x)^\top F'_{\Omega_i}(x) = d_i^2 B^\top (D_i(x))^2 B = d_i^2 B^\top (I_n/d_i^2) B = I_n.$$

**Case (ii):** We have

$$F_{\Omega_i}(x) = \ell_i x + d_i B^\top \sigma \left( Bx + b; \frac{1 - \ell_i}{d_i}, -\frac{1 + \ell_i}{d_i} \right) + c_i$$

and hence

$$\begin{aligned} F'_{\Omega_i}(x)^\top F'_{\Omega_i}(x) &= (\ell_i I_n + d_i B^\top D_i(x) B)^\top (\ell_i I_n + d_i B^\top D_i(x) B) \\ &= \ell_i^2 I_n + d_i^2 B^\top (D_i(x))^2 B + 2\ell_i d_i B^\top D_i(x) B \\ &= B^\top (\ell_i^2 I_n + d_i^2 (D_i(x))^2 + 2\ell_i d_i D_i(x)) B \\ &= B^\top (\ell_i I_n + d_i D_i(x))^2 B = B^\top \tilde{D}_i(x)^2 B \\ &= B^\top B = I_n \end{aligned}$$

where  $D_i(x) \in \mathcal{D}((1 - \ell_i)/d_i, -(1 + \ell_i)/d_i)$  and  $\tilde{D}_i(x) \in \mathcal{D}(\pm 1)$ .

**Verification that (i) and (ii) are the only options:** Let us consider the function  $F$  defined as in (2.1) and restrict to one set  $\Omega_i$  of an arbitrary admissible partition  $\{\Omega_1, \dots, \Omega_N\}$  so that it takes the form

$$F_{\Omega_i}(x) = \ell_i x + c_i + d_i A^\top \sigma_i(Bx + b). \quad (\text{A.1})$$

Since  $\sigma_i : \mathbb{R} \rightarrow \mathbb{R}$  is Lipschitz continuous and piecewise  $C^1$ , so is  $F_{\Omega_i}$ . Thus, Lemma 2.4 allows us to infer that  $\sigma_i$  is piecewise affine.

The Jacobian matrix of (A.1) is

$$F'_{\Omega_i}(x) = \ell_i I_n + d_i A^\top \text{diag}(\sigma'_i(Bx + b)) B = \ell_i I_n + d_i A^\top D_i(x) B,$$

where we set  $D_i(x) = \text{diag}(\sigma'_i(Bx + b))$ . We remark that, despite  $\sigma'_i$  has  $B$  as an input,  $B$  is invertible and hence for any  $y \in \mathbb{R}^n$ , there is  $x \in \mathbb{R}^n$  with  $Bx + b = y$ , and hence we can cover any value of  $\sigma'(\mathbb{R})$  up to properly choosing  $x$ . Such a point  $x$  can be assumed to be in  $\Omega_i$ , since this result must hold for any partition. This allows us to assume  $D_i(x)$  is independent of  $B$ , and, clearly, also independent of  $A$ . The conditions  $F'_{\Omega_i}(x)^\top F'_{\Omega_i}(x) = F'_{\Omega_i}(x) F'_{\Omega_i}(x)^\top = I_n$  write

$$\begin{aligned} (\ell_i^2 - 1) I_n + d_i^2 A^\top (D_i(x))^2 A + \ell_i d_i (A^\top D_i(x) B + B^\top D_i(x) A) &= 0, \\ (\ell_i^2 - 1) I_n + d_i^2 B^\top (D_i(x))^2 B + \ell_i d_i (A^\top D_i(x) B + B^\top D_i(x) A) &= 0. \end{aligned}$$

Subtracting the two conditions above, we get the necessary condition for orthogonality

$$A^\top (D_i(x))^2 A = B^\top (D_i(x))^2 B$$

or, equivalently,

$$(AB^\top)(D_i(x))^2 = (D_i(x))^2(AB^\top). \quad (\text{A.2})$$

We remark that our result must be true for an arbitrary partition  $\{\Omega_1, \dots, \Omega_N\}$  and hence for an arbitrary open and connected set  $\Omega_i \subseteq \mathbb{R}^n$  as well. Since  $A, B \in \mathcal{O}(n)$  are arbitrary orthogonal matrices but they are shared among the sets  $\Omega_1, \dots, \Omega_N$ , we must either have  $AB^\top = P$ , with  $P \in \mathcal{D}(\pm 1)$ , or  $(D_i(x))^2 = b_i I_n$ , for every  $i = 1, \dots, N$ , for almost every  $x \in \mathbb{R}^n$  a suitable choice of  $N$  non-negative scalars  $b_1, \dots, b_N \in \mathbb{R}$ . In fact, if there exists  $i \in \{1, \dots, N\}$  with  $(\sigma'_i(\mathbb{R}))^2$  which is not a singlet, since  $\Omega_i$  is arbitrary, we can assume that for every  $r \neq s$ ,  $r, s \in \{1, \dots, n\}$ , there exists  $\Omega_i \subseteq \mathbb{R}^n$  admitting a positive-measure subregion  $\mathcal{R} \subseteq \Omega_i$  with  $(D_i(x)^2)_{rr} \neq (D_i(x)^2)_{ss}$  for every  $x \in \mathcal{R}$ , hence leading to the constraint that  $AB^\top$  must be diagonal (and orthogonal).

We now consider each case separately and show that they lead to the two forms in the theorem.

**Case  $A = PB$ .** We now have  $F'_{\Omega_i}(x)^\top = F'_{\Omega_i}(x)$  and the orthogonality conditions reduce to

$$(\ell_i I_n + d_i P D_i(x))^2 = I_n. \quad (\text{A.3})$$

Assume  $\ell_i \neq 0$ . Then either  $D_i(x) = 0$  for every  $x \in \mathbb{R}^n$  and for every  $i = 1, \dots, n$ , in which case  $D_i(x)^2 = b_i I_n$  (and we treat it below), or there is an  $i \in \{1, \dots, N\}$  and a positive-measure subregion of  $\mathbb{R}^n$  where  $D_i(x) \neq 0$ . When the second case verifies, either  $P = I_n$  or  $P = -I_n$ . In fact, if  $P$  is any other matrix in  $\mathcal{D}(\pm 1)$ , since the partition is arbitrary, we can assume that there exists a pair of indices  $r \neq s$ ,  $r, s \in \{1, \dots, n\}$ , such that  $P_{rr} = 1 = -P_{ss}$  and  $(D_i(x))_{rr} = (D_i(x))_{ss} \neq 0$  for any  $x \in \mathcal{R}$ ,  $\mathcal{R} \subseteq \Omega_i$  a positive-measure subregion. This leads to a contradiction since it must be true that

$$\begin{aligned} \ell_i + d_i (D_i(x))_{rr} &\in \{\pm 1\}, \\ \ell_i - d_i (D_i(x))_{ss} &= \ell_i - d_i (D_i(x))_{rr} \in \{\pm 1\}. \end{aligned}$$

A necessary condition for this to hold is that  $\ell_i = 0$ , which is not allowed in this configuration.

If  $P = I_n$ , (A.3) together with  $\ell_i \neq 0$  imply that  $D_i(x) \in \mathcal{D}((\pm 1 - \ell_i)/d_i)$ , which fully characterises case (ii). If  $P = -I_n$ , we recover  $D_i(x) \in \mathcal{D}((\pm 1 + \ell_i)/d_i)$ . However, this second situation is equivalent to the former, since we can call  $d'_i = -d_i$  and recover the same condition  $D_i(x) \in \mathcal{D}((\pm 1 - \ell_i)/d'_i)$ , and the layer takes the desired form

$$\begin{aligned} F_{\Omega_i}(x) &= \ell_i x + c_i - d_i B^\top \sigma_i(Bx + b) \\ &= \ell_i x + c_i + d'_i B^\top \sigma_i(Bx + b) \end{aligned}$$

where  $\text{diag}(\sigma'_i(Bx + b)) \in \mathcal{D}((\pm 1 - \ell_i)/d'_i)$ , i.e., case (ii).

Assume, instead,  $\ell_i = 0$ . In this situation, it is enough to have  $d_i D_i(x) \in \mathcal{D}(\pm 1)$ , and hence the condition  $D_i(x) \in \mathcal{D}(\pm 1/d_i)$ , as in case (i), follows. Here, the matrix  $P$  can be kept generic in  $\mathcal{D}(\pm 1)$ , and we recover a particular instance of case (i), since instead of having  $A$  independent from  $B$ , we have it equal to  $PB$ .

**Case  $(D_i(x))^2 = b_i I_n$ .** Here, the orthogonality conditions reduce to the single equation

$$(\ell_i^2 - 1)I_n + b_i d_i^2 I_n + \ell_i d_i (A^\top D_i(x) B + B^\top D_i(x) A) = 0. \quad (\text{A.4})$$

Assume  $\ell_i = 0$ . We recover  $-1 + b_i d_i^2 = 0$  and hence  $b_i = 1/d_i^2$ . This allows us to derive the desired condition, i.e.,  $D_i(x) \in \mathcal{D}(\pm 1/d_i)$ , fully characterising case (i).

Assume, instead,  $\ell_i \neq 0$ . We have

$$A^\top D_i(x) B + B^\top D_i(x) A = k_i I_n$$

where we set  $k_i = -\frac{\ell_i^2 - 1 + b_i d_i^2}{\ell_i d_i}$ . Then, there exists a skew-symmetric matrix valued function  $N_i(\cdot; A, B) : \mathbb{R}^n \rightarrow \mathbb{R}^{n \times n}$ ,  $N_i(x; A, B)^\top = -N_i(x; A, B)$ , possibly depending on  $A$  and  $B$ , such that

$$A^\top D_i(x) B = \frac{k_i}{2} I_n + N_i(x; A, B). \quad (\text{A.5})$$

(A.5) tells us that  $N_i$  depends continuously on the parameters  $A$  and  $B$ , since they appear linearly in the left hand side and it must be true that  $N_i(x; A, B) = A^\top D_i(x)B - k_i/2I_n$ . This condition is equivalent to

$$D_i(x) = \frac{k_i}{2} AB^\top + AN_i(x; A, B)B^\top =: \mathcal{S}(x, A, B). \quad (\text{A.6})$$

We notice that, since the left-hand side of (A.6) is independent of  $A$ , the same should hold for  $\mathcal{S}(x, \cdot, B) : \mathcal{O}(n) \rightarrow \mathbb{R}^{n \times n}$ . In particular, since  $\mathcal{O}(n)$  has two connected components and  $\mathcal{S}(x, A, B)$  is continuous in  $A$ , this means that  $\mathcal{S}(x, \cdot, B)$  is constant on each of these. Let us denote  $SO(n)$  the subset of  $\mathcal{O}(n)$  of those matrices with positive determinants. Thus, without loss of generality we can consider  $B \in SO(n)$  and set  $A = B$ , which gives

$$D_i(x) = \frac{k_i}{2} I_n + BN_i(x; B, B)B^\top.$$

since  $D_i(x) - k_i/2I_n$  is symmetric whereas  $BN_i(x; B, B)B^\top$  is skew-symmetric and similar to  $N_i(x; B, B)$ , we conclude  $N_i(x; B, B) = 0$  for any  $x \in \mathbb{R}^n$  and  $B \in \mathcal{O}(n)$ . Thus

$$D_i(x) = \frac{k_i}{2} I_n$$

which is independent of  $A$  (and  $B$ ) as wanted. Analogously, given  $A = -B \in \mathcal{O}(n) \setminus SO(n)$ , we conclude

$$D_i(x) = -\frac{k_i}{2} I_n.$$

In both cases, we obtain  $b_i = k_i^2/4$ .

On the other hand, (A.5) also implies

$$\begin{aligned} \frac{k_i^2}{4} I_n &= b_i I_n = B^\top D_i(x)^2 B \\ &= (A^\top D_i(x)B)^\top (A^\top D_i(x)B) \\ &= \frac{k_i^2}{4} I - N_i(x; A, B)^2 \end{aligned}$$

and hence  $N_i(x; A, B)^2 = 0$  for every  $A, B \in \mathcal{O}(n)$ . Since

$$N_i(x; A, B)^2 = -N_i(x; A, B)^\top N_i(x; A, B)$$

is symmetric negative semi-definite, and it vanishes, we must have  $N_i(x; A, B) = 0$  for every  $x \in \mathbb{R}^n$  and  $A, B \in \mathcal{O}(n)$  for which (A.5) is true. Substituting back in (A.6), we can obtain that  $A, B \in \mathcal{O}(n)$  satisfy (A.6) if and only if they satisfy

$$D_i(x) = \frac{k_i}{2} BA^\top. \quad (\text{A.7})$$

Since we look for a  $D_i(x)$  independent of  $A$ , the right-hand side of the previous expression must be constant. This solution only exists by setting  $A = PB$  with  $P \in \{I_n, -I_n\}$ , as we also derived in the previous steps of the proof.

Consider the case  $P = I_n$  first. This reasoning implies that, for any  $x \in \mathbb{R}^n$ ,  $D_i(x) \in \mathcal{D}(k_i/2)$ . We conclude that  $\sigma_i : \mathbb{R} \rightarrow \mathbb{R}$  is affine and satisfies

$$d_i \sigma_i(x) = d_i \frac{k_i}{2} x + \mu_i = -\frac{1}{\ell_i} (\ell_i^2 - 1 + b_i d_i^2) x + \mu_i,$$

for a scalar  $\mu_i \in \mathbb{R}$ . On the other hand, if  $P = -I_n$ , we get  $D_i(x) \in \mathcal{D}(-k_i/2)$  and

$$\begin{aligned} d_i \sigma_i(x) &= -d_i \frac{k_i}{2} x + \mu_i = \frac{1}{\ell_i} (\ell_i^2 - 1 + b_i d_i^2) x + \mu_i \\ &= (-d_i) \frac{\ell_i^2 - 1 + b_i (-d_i)^2}{2(-d_i) \ell_i} x + \mu_i = d'_i \frac{k'_i}{2} x + \mu_i \end{aligned}$$

where  $k'_i = -\frac{\ell_i^2 - 1 + b_i (d'_i)^2}{\ell_i d'_i}$  and  $d'_i = -d_i$ , and hence  $D_i(x) \in \mathcal{D}(k'_i/2)$  as desired. Hence, the case  $P = I_n$  encodes all the options.

Since  $(D_i(x))^2 = \frac{k_i^2}{4} I_n$ , i.e.,  $b_i = k_i^2/4$ , the definition of  $k_i$  implies the following equation

$$\frac{k_i^2 d_i^2}{4} + \ell_i^2 + k_i d_i \ell_i = 1.$$

This equation gives  $\frac{k_i}{2} \in \{(\pm 1 - \ell_i)/d_i\}$ , which is coherent with the condition  $D_i(x) \in \mathcal{D}((\pm 1 - \ell_i)/d_i)$  obtained for the case  $A = PB$  and  $\ell_i \neq 0$ , but is just a particular case since here we get affine maps. We remark that for this choice of  $\sigma_i$ , the map  $F$  restricted to  $\Omega_i$  writes

$$F_{\Omega_i}(x) = \ell_i x + c_i + (p_i - \ell_i)x + v_i = p_i x + c_i + \mu_i B^\top b$$

for an arbitrary pair of scalars  $\mu_i \in \mathbb{R}$  and  $p_i \in \{\pm 1\}$ .

## B Proof of Corollary 2.9

We focus on a generic  $\Omega_i \subset \mathbb{R}^n$ , and consider

$$G_{\Omega_i}(x) = \ell_i O x + c_i + d_i A^\top \sigma_i(B x + b).$$

Calling  $y = y(x) = O x$ , we see that, by the orthogonality of  $O$ , it follows that

$$G_{\Omega_i}(x) = \ell_i O x + c_i + d_i A^\top \sigma_i(B O^\top O x + b) = \widehat{G}_{\Omega_i}(y(x))$$

with

$$\widehat{G}_{\Omega_i}(y) = \ell_i y + c_i + d_i A^\top \sigma_i(B O^\top y + b).$$

Recall that  $G_{\Omega_i}$  has an orthogonal Jacobian matrix if and only if

$$G'_{\Omega_i}(x)(G'_{\Omega_i}(x))^\top = I_n = (G'_{\Omega_i}(x))^\top G'_{\Omega_i}(x).$$

Equivalently, by the chain rule, we get

$$\begin{aligned} I_n &= \widehat{G}'_{\Omega_i}(y(x)) y'(x) y'(x)^\top (\widehat{G}'_{\Omega_i}(y(x)))^\top, \\ I_n &= y'(x)^\top (\widehat{G}'_{\Omega_i}(y(x)))^\top \widehat{G}'_{\Omega_i}(y(x)) y'(x). \end{aligned}$$

Since  $y'(x) = O$  is orthogonal, the two conditions are equivalent to  $\widehat{G}'_{\Omega_i}(y)$  being orthogonal almost everywhere. Since  $\widehat{B} := B O^\top$  is orthogonal as well,  $\widehat{G}_{\Omega_i}$  has the same form as case (ii), which leads to the condition  $A = B O^\top$ , as desired. Thus, we conclude that

$$\begin{aligned} G_{\Omega_i}(x) &= \ell_i O x + c_i + d_i O B^\top \sigma_i(B x + b) \\ &= O(\ell_i x + c_i + d_i B^\top \sigma_i(B x + b)) \\ &= O F_{\Omega_i}(x) \end{aligned}$$

as desired.

## C Proof of Theorem 4.1

The proof presented for  $\sigma(x; \alpha, \beta) = \max\{\alpha x, \beta x\}$  extends to a generic continuous piecewise affine activation  $\sigma(x; \alpha, \beta)$  and we now show such a generalisation.

We start by introducing a generic characterisation of the activation functions we are considering.

**LEMMA C.1** (Theorem 4.1 in [34]). Let  $\sigma : \mathbb{R} \rightarrow \mathbb{R}$  be a continuous piecewise affine function. Then, there exists a  $k \in \mathbb{N}$ , and a choice of scalars  $a_{i,j}, b_{i,j} \in \mathbb{R}$ ,  $i = 1, \dots, k$ ,  $j = 1, \dots, \ell_i$ , such that

$$\sigma(x) = \max\{\sigma^1(x), \dots, \sigma^k(x)\}, \tag{C.1}$$

where, for every  $i = 1, \dots, k$ , we set

$$\sigma^i(x) = \min\{a_{i,1}x + b_{i,1}, \dots, a_{i,\ell_i}x + b_{i,\ell_i}\}.$$

For an activation  $\sigma \in \mathcal{L}(\alpha, \beta)$ ,  $\alpha, \beta \in \mathbb{R}$ , it is immediate to see that  $a_{i,j} \in \{\alpha, \beta\}$  for every  $i = 1, \dots, k$  and  $j = 1, \dots, \ell_i$ . In such a case, we recall the notation  $\sigma(\cdot) = \sigma(\cdot; \alpha, \beta)$ .

Assume now  $\Omega$  is compact, and consider an activation function  $\sigma$  as in (C.1) with slopes limited to a set of two elements. Fix  $\varepsilon > 0$  and two continuous functions  $m, q : \Omega \rightarrow \mathbb{R}$ . Call  $M_\Omega := \max_{x \in \Omega} \|x\|_2$  and consider a finite collection of sets  $\{\Omega_1, \dots, \Omega_N\}$  in  $\mathcal{P}(\Omega)$  such that

$$\begin{aligned} \max_{x \in \Omega} |m(x) - \tilde{m}(x)| &\leq \frac{\varepsilon}{4\sqrt{n}(M_\Omega\sqrt{n} + \|b\|_2)}, \\ \max_{x \in \Omega} |q(x) - \tilde{q}(x)| &\leq \frac{\varepsilon}{2}, \end{aligned}$$

where  $\tilde{m}, \tilde{q} : \Omega \rightarrow \mathbb{R}$  are piecewise constant approximations of  $m$  and  $q$ , which are constant on each of the sets  $\Omega_1, \dots, \Omega_N$ .

Consider now the two functions  $\mathcal{F}_\Omega(x; m, q)$  and  $\mathcal{F}_\Omega(x; \tilde{m}, \tilde{q})$  and write the difference

$$\begin{aligned} \mathcal{F}_\Omega(x; m, q) - \mathcal{F}_\Omega(x; \tilde{m}, \tilde{q}) &= (m(x) - \tilde{m}(x))x + (q(x) - \tilde{q}(x)) \\ &\quad + 1_\Omega(x)B^\top \left( \sigma(Bx + b; 1 - m(x), -1 - m(x)) \right. \\ &\quad \left. - \sigma(Bx + b; 1 - \tilde{m}(x), -1 - \tilde{m}(x)) \right). \end{aligned}$$

We now explicitly write the two functions whose difference needs to be controlled:

$$\begin{aligned} \mathcal{S} &:= \sigma(Bx + b; 1 - m(x), -1 - m(x)) = \max_{i=1, \dots, k} \min_{j=1, \dots, \ell_i} (a_{i,j}(x)(Bx + b) + b_{i,j}) \\ \tilde{\mathcal{S}} &:= \sigma(Bx + b; 1 - \tilde{m}(x), -1 - \tilde{m}(x)) = \max_{i=1, \dots, k} \min_{j=1, \dots, \ell_i} (\tilde{a}_{i,j}(x)(Bx + b) + b_{i,j}). \end{aligned}$$

Since the expression based on  $\tilde{m}$  and  $\tilde{q}$  can be constructed specifically for the target function at hand, we can assume that  $a_{i,j}$  and  $\tilde{a}_{i,j}$  have agreeing expressions, meaning that if  $a_{i,j}(x) = 1 - m(x)$ , then  $\tilde{a}_{i,j}(x) = 1 - \tilde{m}(x)$ , for example. It follows that, for any  $x \in \Omega$ , one has

$$\begin{aligned} \|\mathcal{S} - \tilde{\mathcal{S}}\|_\infty &= \max_{r=1, \dots, n} |\sigma((Bx + b)_r; 1 - m(x), -1 - m(x)) - \sigma((Bx + b)_r; 1 - \tilde{m}(x), -1 - \tilde{m}(x))| \\ &\leq \max_{r=1, \dots, n} \max_{i,j} |(a_{i,j}(x) - \tilde{a}_{i,j}(x))(Bx + b)_r| = \max_{i,j} \max_{r=1, \dots, n} |(a_{i,j}(x) - \tilde{a}_{i,j}(x))(Bx + b)_r| \\ &= \max_{i,j} \|(a_{i,j}(x) - \tilde{a}_{i,j}(x))(Bx + b)\|_\infty \leq \left( \max_{i,j} |a_{i,j}(x) - \tilde{a}_{i,j}(x)| \right) \|Bx + b\|_\infty, \end{aligned}$$

where  $a_{i,j}(x) \in \{1 - m(x), -1 - m(x)\}$ ,  $\tilde{a}_{i,j}(x) \in \{1 - \tilde{m}(x), -1 - \tilde{m}(x)\}$ , and  $b_{i,j} \in \mathbb{R}$ . This means that

$$\max_{i,j} |a_{i,j}(x) - \tilde{a}_{i,j}(x)| \leq |m(x) - \tilde{m}(x)| \leq \frac{\varepsilon}{4\sqrt{n}(M_\Omega\sqrt{n} + \|b\|_2)}.$$

Thus, it follows that

$$\|\mathcal{S} - \tilde{\mathcal{S}}\|_\infty \leq \sqrt{n} \frac{\varepsilon}{4\sqrt{n}(M_\Omega\sqrt{n} + \|b\|_2)} (M_\Omega\sqrt{n} + \|b\|_2) = \frac{\varepsilon}{4}.$$

We then obtain the desired result

$$\begin{aligned} \max_{x \in \Omega} \|\mathcal{F}_\Omega(x; m, q) - \mathcal{F}_\Omega(x; \tilde{m}, \tilde{q})\|_\infty &\leq \frac{\varepsilon}{4\sqrt{n}(M_\Omega\sqrt{n} + \|b\|_2)} M_\Omega + \frac{\varepsilon}{2} + \frac{\varepsilon}{4} \\ &\leq \frac{\varepsilon}{4} + \frac{\varepsilon}{2} + \frac{\varepsilon}{4} = \varepsilon \end{aligned}$$

as desired, where we used the estimate

$$\begin{aligned} \|(m(x) - \tilde{m}(x))x\|_\infty &\leq \max_{x \in \Omega} |m(x) - \tilde{m}(x)| \|x\|_2 \\ &\leq \frac{\varepsilon}{4\sqrt{n}(M_\Omega\sqrt{n} + \|b\|_2)} M_\Omega \\ &\leq \frac{\varepsilon\sqrt{n}(M_\Omega\sqrt{n} + \|b\|_2)}{4\sqrt{n}(M_\Omega\sqrt{n} + \|b\|_2)} = \frac{\varepsilon}{4}. \end{aligned}$$

This allows us to conclude the proof.

## D Experimental setup

In Section 5, we use convolutional networks and minimise the cross-entropy loss function. Our theory targets layers that preserve the number of channels or the input dimension, like those in ResNets. When an expansion is needed, we add zero channels. After the convolutional layers we flatten the output and feed it to a trainable randomly initialized linear classifier. We include regularisation terms in the loss function to promote the necessary weight orthogonality. The regularisation term is the one proposed in [47], which is the equivalent of  $\mathcal{R}(A) = \alpha \|AA^\top - I\|_F$  for convolutional layers, to promote the orthogonality of the matrix representation of the convolution operation on flattened images. We report results for  $\alpha = 0.001$  and  $\alpha = 0$  to test the hypothesis that orthogonality at initialisation is enough for the network trainability.

All models are trained using the Adam optimiser with a cosine decay learning rate scheduler. For the experiments with 50 and 200 layers we vary the learning rate in  $[10^{-5}, 5 \cdot 10^{-5}]$ , whereas for those with 10 layers in  $[10^{-4}, 5 \cdot 10^{-4}]$ . We use batches of size 512 and comment on the timings per training iterate in Appendix E. Early stopping occurs when no improvement is observed within a sliding window of training epochs. We set a patience of 10 epochs, with a maximum number of epochs set to 400. Our experimental analysis does not include feedforward networks with weights initialised as random normal, as they are well known to suffer from vanishing gradient problems, rendering them impossible to train.

## E Computational efficiency and timings

We trained our models on NVIDIA Quadro RTX 6000 GPUs with 24GB of RAM. We report in Table 3 the training times of the various models tested in the Section 5. The timing corresponds to the time per point in the batch. As expected, the models have a training time that grows with the number of layers. We observe the steepest growth for the regularised feedforward and limit models. It is also inevitable that, having the limit model with  $m_3$  more parameters than the others, it requires more time per iteration. In the model column, we denote with FF the feedforward networks.

In terms of memory, most models have comparable costs to conventional ones. In contrast, models relying on activation functions with more than two affine pieces, such as  $\sigma_3$  and  $\text{ReLU}_3$ , are more memory intensive.

## F Proof that the considered models are partial isometries

Let us consider models as in case (i), with  $\sigma \in \mathcal{L}(-1, 0, 1)$ . Then, we notice that the Jacobian matrix at  $x$ , a point where the layer is differentiable, writes

$$J(x) = A^\top \text{diag}(\sigma'(Bx + b))B =: A^\top D(x)B, \quad D(x) \in \mathcal{D}(-1, 0, 1).$$

This implies that

$$J(x)J(x)^\top = A^\top D(x)^2 A,$$

and hence

$$(J(x)J(x)^\top)^2 = A^\top D(x)^4 A.$$

To have the desired partial orthogonality, we thus need  $D^2(x) = D^4(x)$  to hold, or, equivalently, that  $D^2(x)(D^2(x) - I) = 0$ . This condition holds if and only if each entry  $D_{ii}(x)$  is either  $-1, 0$  or  $1$ . We remark that this happens when  $\sigma(x) = \text{ReLU}(x)$  as considered in Section 5. If  $\sigma(x) = \max\{0.3x, x\}$ , as in the LeakyReLU experiments we considered, then  $D_{ii}(x) \in \{0.3, 1\}$ . Here, we do not exactly satisfy the partial orthogonality condition. Still, we see that  $D_{ii}(x)^2 \in \{1, 0.09\}$ , so the partial orthogonality conditions are almost satisfied.

Similarly, for the models based on case (ii), if  $\sigma \in \mathcal{L}(0, 1, 2)$  we get the desired partial orthogonality of the Jacobian, when well defined. This is because the Jacobian writes

$$J(x) = I_n - B^\top \text{diag}(\sigma'(Bx + b))B =: I_n - B^\top D(x)B.$$

It follows that

$$J(x)J(x)^\top = I_n + B^\top D(x)^2 B - 2B^\top D(x)B = B^\top (I_n + D(x)^2 - 2D(x))B. \quad (\text{F.1})$$

Table 3: Timings of the trained models (average milliseconds per data point). Average training times for the considered models reported as time per data point in the batch. We vary the number of layers  $L \in \{10, 50, 200\}$ , and the orthogonal regularisation parameter  $\alpha \in \{0, 0.001\}$ .  $\alpha = 0$  corresponds to orthogonal initialisation with no regularisation. The first column indicates the architecture type and the activation function. Each number represents the average over the epochs. The term after  $\pm$  gives the interval to which the results belong.

Model	$\alpha$	10	50	200
FF- $\sigma_1$	0	1.75 $\pm$ 0.94	6.86 $\pm$ 3.40	26.62 $\pm$ 12.92
	0.001	2.50 $\pm$ 0.91	10.62 $\pm$ 3.54	41.29 $\pm$ 13.32
FF- $\sigma_3$	0	2.44 $\pm$ 1.09	10.42 $\pm$ 4.65	40.76 $\pm$ 18.98
	0.001	3.54 $\pm$ 1.57	13.98 $\pm$ 4.92	55.41 $\pm$ 18.98
ResNet-ReLU	0	1.52 $\pm$ 0.77	5.81 $\pm$ 2.79	21.96 $\pm$ 10.09
	0.001	1.87 $\pm$ 0.80	7.65 $\pm$ 2.87	29.83 $\pm$ 11.94
ResNet-ReLU <sub>3</sub>	0	1.56 $\pm$ 0.78	5.76 $\pm$ 2.68	21.97 $\pm$ 9.95
	0.001	1.91 $\pm$ 0.81	7.61 $\pm$ 2.83	29.56 $\pm$ 10.75
ResNet <sub>B</sub>	0	1.58 $\pm$ 0.66	5.93 $\pm$ 2.87	22.36 $\pm$ 10.74
	0.001	1.95 $\pm$ 0.70	7.65 $\pm$ 2.87	29.31 $\pm$ 10.16
FF-ReLU	0	1.79 $\pm$ 0.77	7.11 $\pm$ 3.43	26.95 $\pm$ 12.36
	0.001	2.52 $\pm$ 0.69	10.66 $\pm$ 3.18	41.52 $\pm$ 12.62
FF-Leaky ReLU	0	1.82 $\pm$ 0.78	7.09 $\pm$ 3.35	27.11 $\pm$ 12.38
	0.001	2.54 $\pm$ 0.68	10.68 $\pm$ 3.18	41.66 $\pm$ 12.70
$m_2$	0	2.26 $\pm$ 1.07	9.24 $\pm$ 4.95	35.93 $\pm$ 18.13
	0.001	2.62 $\pm$ 1.23	11.15 $\pm$ 4.93	43.86 $\pm$ 19.35
$m_3$	0	3.17 $\pm$ 1.57	14.20 $\pm$ 6.90	55.91 $\pm$ 25.92
	0.001	3.59 $\pm$ 1.59	16.08 $\pm$ 6.61	63.73 $\pm$ 27.14

Then, considering its square, we recover

$$\begin{aligned}
 (J(x)J(x)^\top)^2 &= B^\top(I_n + D(x)^2 - 2D(x))^2 B \\
 &= J(x)J(x)^\top \\
 &= B^\top(I_n + D(x)^2 - 2D(x))B,
 \end{aligned}$$

where the second inequality comes by (F.1).

We conclude that

$$(I_n + D(x)^2 - 2D(x))D(x)(D(x) - 2I_n) = 0.$$

This translates to a condition on the diagonal entries of  $D(x)$ , which must either be 0, or 2, or solve

$$1 + D_{ii}^2(x) - 2D_{ii}(x) = (1 - D_{ii}(x))^2 = 0.$$

We conclude that the allowed options are  $D_{ii}(x) \in \{0, 1, 2\}$ , and hence  $\sigma \in \mathcal{L}(0, 1, 2)$ . This is satisfied by  $\sigma(x) = \text{ReLU}(x)$ , which is the one tested in Section 5.